*Int. J. Electrochem. Sci.*, 11 **(2016)** 6747 – 6760, doi: 1020964/2016.08.01

**International Journal of ELECTROCHEMICAL SCIENCE**
www.electrochemsci.org

# Facile Synthesis of NiO/CuO/reduced Graphene Oxide Nanocomposites for Use in Enzyme-free Glucose Sensing

*Su-Juan Li*[*], *Yun Xing, Lin-Lin Hou, Zhu-Qing Feng, Yu Tian, Ji-Min Du*

Henan Province Key Laboratory of New Optoelectronic Functional Materials, College of Chemistry and Chemical Engineering, Anyang Normal University, Anyang, 455000, Henan, China.
[*]E-mail: lemontree88@163.com

*Received:* 26 April 2016 / *Accepted:* 21 May 2016 / *Published:* 7 July 2016

In this work, reduced graphene oxide (rGO) supported biocatalyst of NiO/CuO nanocomposites were prepared on glassy carbon electrode (GCE) through a facile and direct electrochemical method. Scanning electron microscopy, energy dispersive X-ray spectroscopy (EDX) and electrochemical techniques were used to characterize the obtained modified electrode. In alkaline solution, the NiO/CuO/rGO nanocomposites exhibited superior electrocatalytic performance to glucose oxidation compared to monometallic oxide counterparts of NiO/rGO and CuO/rGO. The influences of NaOH concentration, duration time for electrodeposition, and applied potential on the amperometric responses of glucose were optimized. Under optimal conditions, the amperometric sensor demonstrated the wide linear range (5 μM-4.85 mM), high sensitivity (1046 μA $mM^{-1}$ $cm^{-2}$), low detection limit (0.5 μM) and good selectivity to glucose determination.

**Keywords:** Electrodeposition, Copper oxide, Nickle oxide, Graphene, Glucose

## 1. INTRODUCTION

Glucose biosensor has gained special focus for decades [1-4], not only due to the rising demands for blood glucose detection but also important for control of bioprocess and pharmaceutical analysis. The enzyme based electrochemical biosensors, which were pioneered by Clark and Lyons [5], are often used for glucose sensing. However, these enzyme based sensors involve several disadvantages, including the high price of enzymes, complex immobilization processes and poor stability [6-8]. To overcome such limitations, great efforts have been focused on developing enzyme-free glucose biosensors.

Recently, various materials, such as noble metals (Pd, Pt, Au) [9-11], metal alloys [12,13] and oxides (NiO, CuO, $Co_3O_4$, $Cu_2O$) [14-18] have been widely used as electrode modifications for enzyme-free glucose sensing. Unfortunately, noble metals including Pt and Au often suffer from

sluggish kinetics for glucose oxidation, and their surfaces are easily poisoned by adsorbed $Cl^-$ and intermediates. Therefore, metal oxides are attracting growing interest in practical enzyme-free glucose biosensors thanks to their low cost and resourceful features. Especially, when two different metals or their oxides were integrated together to form a novel binary electrocatalyst, such as $MnO_x/NiO_x$ [19], $Cu_2O$/NiOx [20] and Ni-Co nanostructures [21], it is reported that their electrocatalytic activities and anti-interference abilities for glucose electrooxidation were significantly enhanced compared to their monometallic counterparts. In this work, biocatalyst of Cu and Ni oxides has deserved a special attention. Due to their facile synthesis, high electrocatalytic activity and prominent redox properties, they have potential for application in enzyme-free glucose sensing.

For improving the catalytic activity of these metal oxides, various carbon materials were often used as support matrix to promote the charge transfer [14,16,20-22]. Graphene, a typical two dimensional carbon material, is commonly used for catalyst support due to its unique structure and outstanding electrical conductivity [23,24]. In recent years, growing interest of researchers have been committed to the design of novel functional materials incorporated with graphene to improve electrochemical performances. Several graphene supported catalyst nanocomposites, including graphene/metal or metal oxide [25], graphene/prussian blue [26], graphene/quantum dots [27], and graphene/conducting polymers [28] have been reported.

We prepared reduced graphene oxide (rGO) supported binary catalyst of NiO/CuO nanocomposites by scanning the potential of the GO modified electrode in deposition solutions involved with $NiSO_4$ and $CuSO_4$ at a constant cathodic potential. In this process, nickel and copper ions were first reduced to metallic state, forming Ni/Cu along the surface of GO. Simultaneously, GO was reduced to rGO at this cathodic potential. Then, the resultant electrode was scanned in NaOH solution by cyclic voltammetry (CV) to oxide metallic Ni/Cu and thus NiO/CuO/rGO modified electrode was obtained. The electrocatalytic performances of the present NiO/CuO/rGO modified electrode for oxidation of glucose were investigated. It was found that the developed enzyme-free glucose sensor have wide linear range, low detection limit, high sensitivity and acceptable selectivity.

## 2. EXPERIMENTAL SECTIONE

### *2.1. Reagents and apparatus*

GO was purchased from Nanjing XFNANO Materials Tech Co., Ltd (China). 10 mg of the obtained GO was dispersed in 10 mL water to give a 1 mg $mL^{-1}$ brown dispersion for use. Glucose, fructose, lactose, dopamine (DA), ascorbic acid (AA), and uric acid (UA) were purchased from Sigma-Aldrich. $CuSO_4.5H_2O$, $NiSO_4$, NaOH and $H_2O_2$ were purchased from Sinopharm Chemical Reagent Co., Ltd (Shanghai, China). The supporting electrolyte used for electrodeposition was 0.1 M pH 4.0 acetate buffer solutions (ABS), prepared using HAc and NaAc. Other reagents were of analytical grade and used as received. Ultrapure water (18.2 MΩ cm) produced from a Milli-Q system was used for preparing aqueous solutions.

Scanning electron microscopy (SEM) equipped with an energy-dispersive X-ray spectroscopy (EDX) analyzer was conducted by Hitachi SU8010 (Japan) for characterization of surface morphology

of modified electrode. Electrochemical measurements were carried out on a CHI 660D electrochemical station (Shanghai Chenhua, China) with a conventional three-electrode system, involving the NiO/CuO/rGO modified glassy carbon electrode (NiO/CuO/rGO/GCE) as the working electrode, a Pt wire as counter electrode and a saturated calomel electrode (SCE) as reference electrode.

### *2.2. Preparation of NiO/CuO/rGO nanocomposites electrode*

The glassy carbon electrode (GCE) was pretreated by polishing with 0.3 and 0.05 μm alumina slurries, and successively ultrasonicated in ethanol and double distilled water. 10 μL of the obtained GO dispersion was modified on the polished GCE and allowed to dry in air to obtain GO/GCE. Then, the GO/GCE was immersed into a deposition solution involving 0.1 M ABS + 5 mM $NiSO_4$ + 5 mM $CuSO_4$ and then -1.0 V of the applied potential was exerted on the electrode for 240 s to electrodeposition of Ni-Cu nanoparticles. Under this applied potential, GO was also electrochemically reduced to rGO, forming the Ni/Cu/rGO nanocomposites. At last, for oxidizing Ni/Cu nanoparticles to be NiO/CuO, the Ni/Cu/rGO modified electrode was scanned in 0.1 M NaOH for 20 cycles by CV technique in the potential range of -0.50~0.30 V at 50 mV $s^{-1}$. The resultant electrode was defined to be NiO/CuO/rGO/GCE. The electrodeposition process for preparation of NiO/CuO/rGO/GCE is illustrated in Scheme 1. For comparison, NiO/rGO/GCE and CuO/rGO/GCE were prepared with the above described procedures except the deposition solutions of 0.1 M ABS + 10 mM $NiSO_4$ and 0.1 M ABS + 10 mM $CuSO_4$, respectively. The rGO/GCE was prepared by electroreduction of the GO/GCE in 0.1 M ABS at a potential of -1.0 V for 240 s.

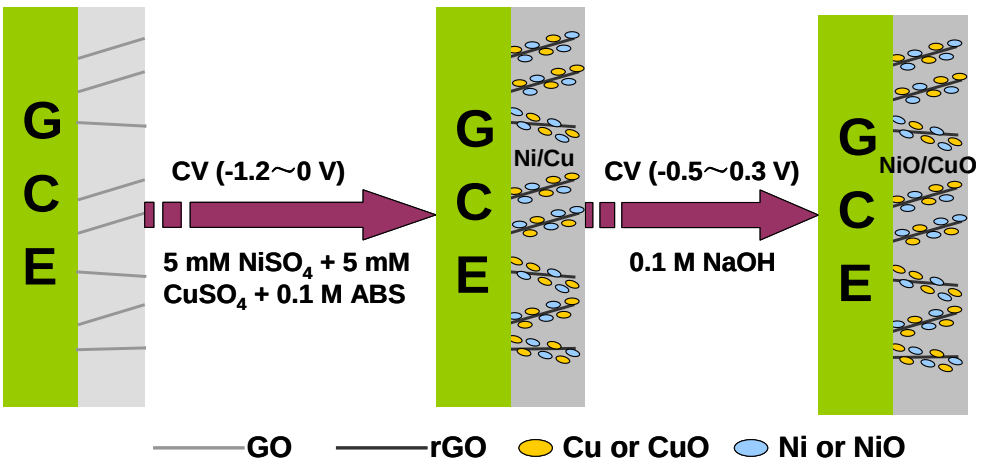


**Scheme 1**. Schematic illustration for the fabrication of NiO/CuO/rGO/GCE.

## 3. RESULTS AND DISCUSSION

### *3.1. Formation mechanism and characterization of the NiO/CuO/rGO nanocomposites electrode*

It has been reported that GO can be electrochemically reduced to rGO by applying a constant cathodic potential [29,30]. The cation of $Ni^{2+}$ and $Cu^{2+}$ can also electrochemically converted to

metallic nickel and copper [17,31]. Based on these results, a direct electrodeposition method was utilized to prepare NiO/CuO/rGO nanocomposites electrode by using GO precursor. Typically, a GO/GCE was employed in pH 4.0 ABS containing $NiSO_4$ and $CuSO_4$ using a constant potential of -1.0 V. Under this potential, $Ni^{2+}$ and $Cu^{2+}$ could be reduced at GO surface; simultaneously, GO has been reduced to rGO. Then, the obtained Ni/Cu/rGO electrode was subjected to electrochemical scanning in alkaline solution using CV, allowing the formation of NiO/CuO/rGO/GCE.

Electrochemical properties of the resultant NiO/CuO/rGO/GCE has been investigated in 0.1 M NaOH using CV. As shown in Fig.1, the anodic and cathodic scans display three obvious oxidation and reduction peaks. The oxidation peaks at potentials of -0.355 (a) and -0.158 V (b) are attributed to the oxidation of Cu to $Cu^+$ and of $Cu^+$ to $Cu^{2+}$, respectively. The reduction peaks at potentials of -0.602 (b') and -0.869 V (a') represent the transition of $Cu^{2+}$ to $Cu^+$ and of $Cu^+$ to Cu, respectively. These results are consistent with those previously reported for Cu based materials [32]. Besides the typical redox peaks of CuO, the redox peak located at 0.545 (c) and 0.342 V (c') can be assigned to the $NiO+OH^- - e \rightarrow NiOOH$ reaction [33]. Therefore, the CV results revealed the successful formation of NiO/CuO on rGO surface and also validated that the deposited NiO/CuO exhibited their characteristic electrochemical behaviors.

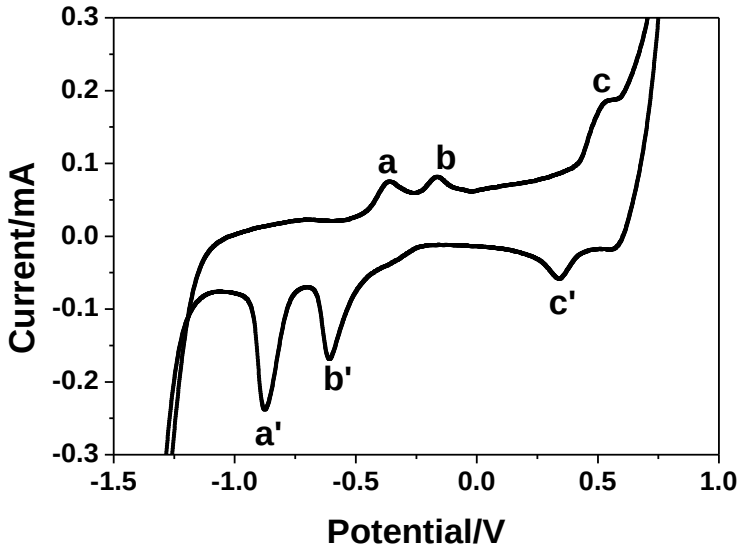


**Figure 1.** CV of NiO/CuO/rGO/GCE in 0.1 M NaOH at 50 mV $s^{-1}$.

The morphology of the synthesized materials on electrode surface was characterized by SEM. Fig. 2 shows SEM images of rGO/GCE (a), CuO/rGO/GCE (b), NiO/rGO/GCE (c) and NiO/CuO/rGO/GCE (d). As observed, the rGO/GCE shows a typical wrinkled structure with plenty of corrugations and scrolling [34]. For CuO/rGO/GCE, huge amounts of thick and compact CuO nanoparticles with diameters of several hundred nanometers agglomerate tightly on electrode surface, which is unbeneficial for mass and electron transport.

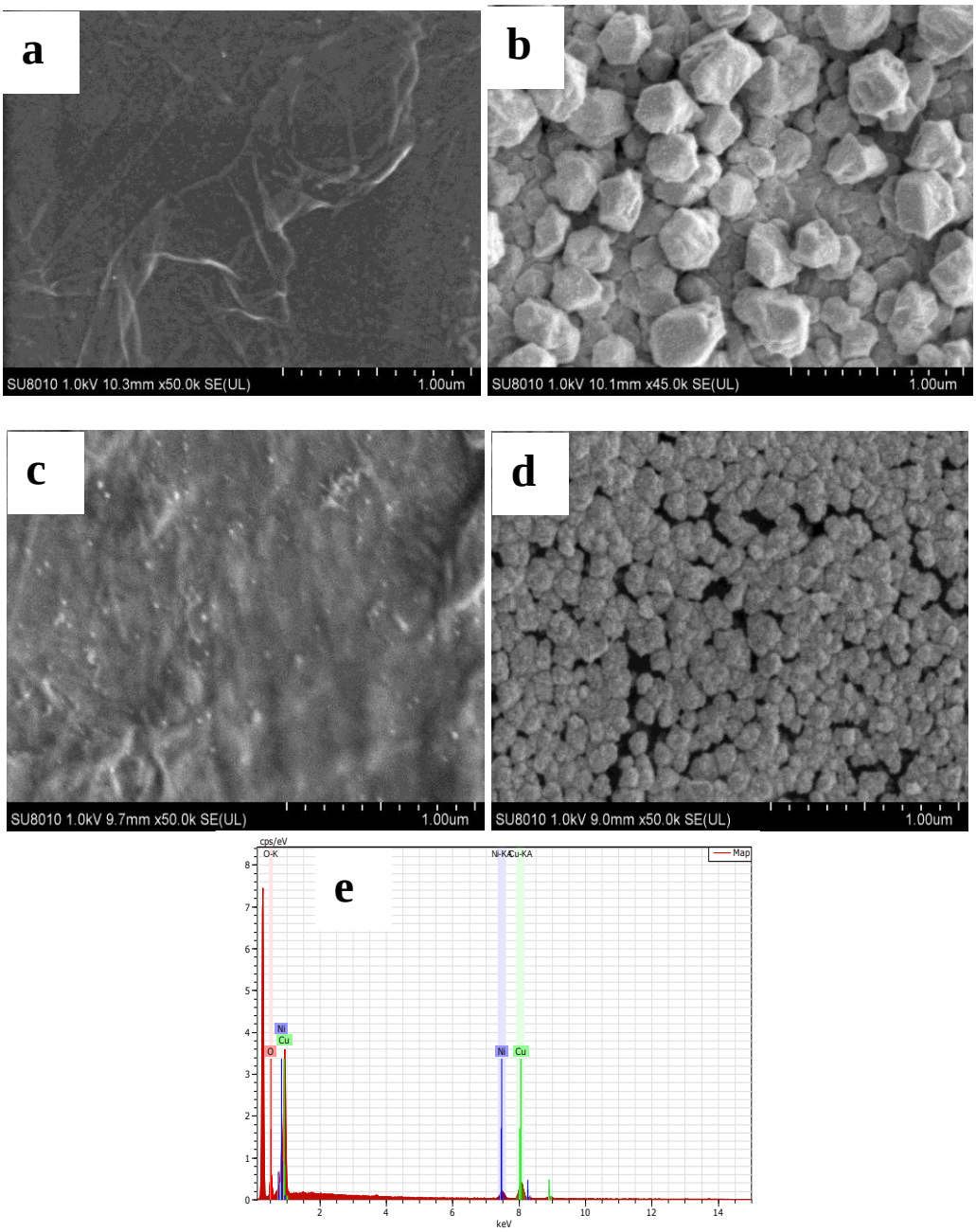


**Figure 2.** SEM images of rGO/GCE (a), CuO/rGO/GCE (b), NiO/rGO/GCE (c) and NiO/CuO/rGO/GCE (d). Fig.2e is the EDX spectra of NiO/CuO/rGO/GCE.

The NiO/rGO/GCE shows small NiO nanoparticles with diameters of 10-20 nm uniformly distributed on wrinkled rGO surface. The image of NiO/CuO/rGO/GCE indicates that a large amount of NiO/CuO nanoparticles with diameters of 50～200 nm are homogeneously distributed on surface of rGO. The NiO/CuO/rGO/GCE with high loading amount of efficient biocatalyst combines the electrocatalytic activities of two promising components. The EDX spectra of NiO/CuO/rGO/GCE, as demonstrated in Fig. 1e, shows that elements of C, O, Cu and Ni obtained, suggesting the successful formation of NiO/CuO nanocomposites on rGO surface.

*3.2. Enhanced electrochemical oxidation of glucose on NiO/CuO/rGO/GCE*

We investigated the electrocatalytic property of NiO/CuO/rGO/GCE toward glucose oxidation. Fig. 3 presents the CVs of electrodes modified with rGO, CuO/rGO, NiO/rGO, and NiO/CuO/rGO in 0.1 M NaOH without and with 2 mM glucose involved. As can be seen, the electrocatalytic oxidation current of glucose on rGO/GCE (Fig. 3a) is observed from a potential of 0.5 V. The high required potential will result in sluggish electrode kinetic for glucose oxidation. The CuO/rGO/GCE (Fig. 3b) shows a reduction peak at 0.57 V in NaOH solution, assigning to $CuOOH+e \rightarrow CuO+OH^-$ reaction. The oxidation peak corresponding to conversion of CuO to CuOOH was not clearly observed, probably covered with the anodic peak of water-splitting [35]. Upon addition of 2 mM glucose, an obvious anodic current increase at starting potential of 0.20 V was observed at CuO/rGO/GCE due to electrocatalytic oxidation of glucose by CuO nanoparticles (CuOOH+glucose→CuO+gluconolactone). For NiO/rGO/GCE (Fig. 3c), a pair of redox peaks located at 0.47/0.34 V in NaOH electrolyte can be assigned to the $NiO+OH^- - e \rightarrow NiOOH$ reaction, the obtained NiOOH electrocatalyzed the oxidation of glucose (NiOOH+glucose→NiO+gluconolactone), giving rise to an increased anodic peak current at starting potential of 0.30 V. In contrast, the NiO/CuO/rGO/GCE (Fig. 3d) with binary catalyst displays both the characteristic peaks of NiO and CuO in NaOH solution.

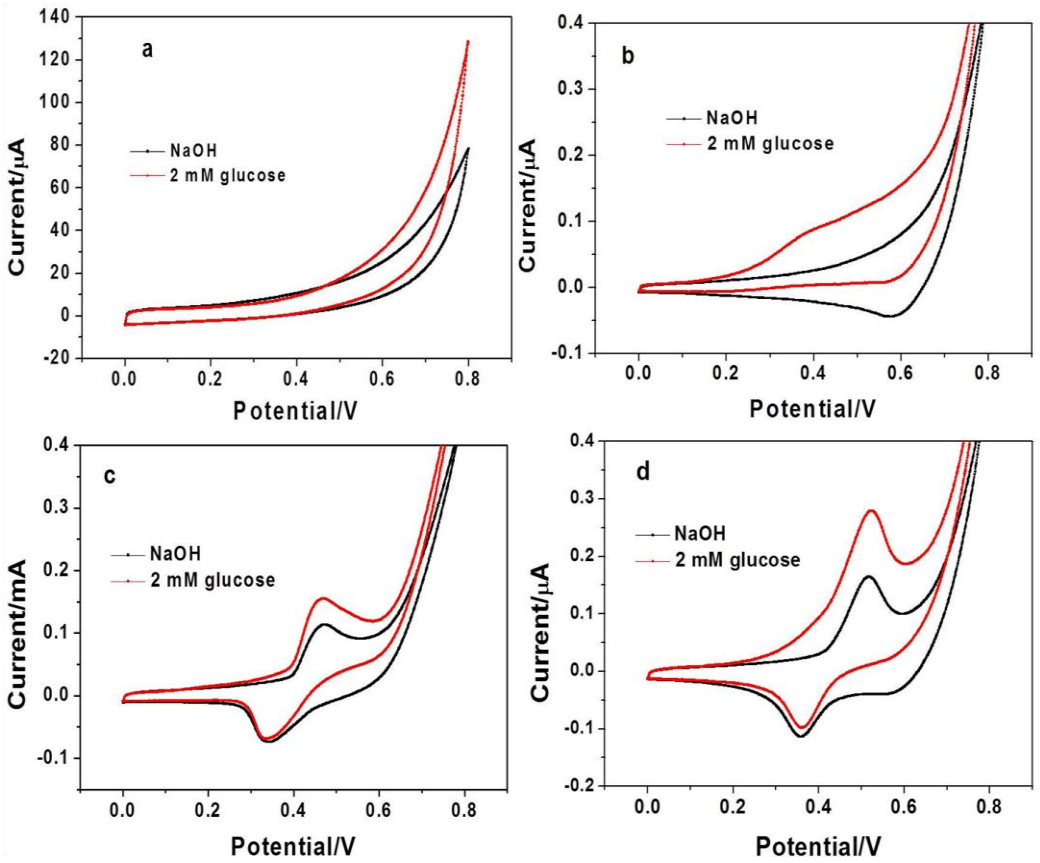


**Figure 3.** CVs of rGO/GCE (a), CuO/rGO/GCE (b), NiO/rGO/GCE (c) and NiO/CuO/rGO/GCE (d) in 0.1 mol $L^{-1}$ NaOH without (black curve) and with (red curve) 2 mM glucose involved at a scan rate of 50 mV $s^{-1}$.

A distinct enhancement of the anodic current at onset potential of 0.24 V upon the addition of glucose is distinctly observed. The oxidation peak currents were found to be proportional to the square root of scan rate, demonstrating a diffusion-dominated electron transfer process for electrocatalytic oxidation of glucose. Compared the CV response of the above four electrodes to glucose, it can be observed that the NiO/CuO/rGO/GCE showed the largest electrocatalytic oxidation current. Meanwhile, the onset oxidation potential of 0.24 V for glucose at NiO/CuO/rGO/GCE is more negative than 0.30 V of NiO/rGO/GCE. All these phenomenons suggest that the biocatalyst of NiO/CuO loaded on rGO surface facilitate the glucose oxidation probably because of the synergistic effect of NiO and CuO.

To further validate the superior ectrocatalytic activity of NiO/CuO/rGO nanocomposites toward glucose oxidation, the amperometric responses of the above four electrodes to successive injections of 50 μM glucose in trirred NaOH solution were performed at 0.5 V. The results are shown in Fig 4. Obviously, NiO/CuO/rGO/GCE responds to glucose with the largest amperometric current, compare to the other three electrodes. The enhanced performance of the NiO/CuO/rGO nanocomposites benefits from a coordination effect between electrocatalysts of NiO and CuO, which contains more electroactive sites for oxidation of glucose. Furthermore, the homogeneous distribution of NiO/CuO nanoparticles and high conductivity of rGO contributes to the enhanced electrooxidation of glucose.

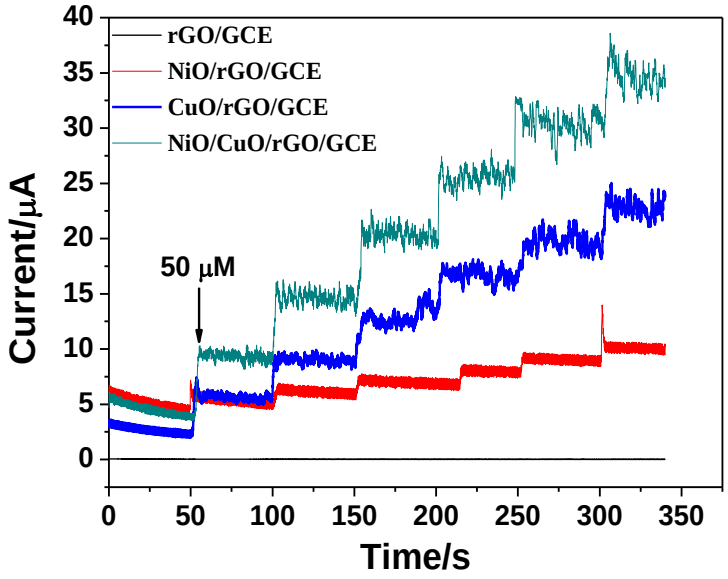


**Figure 4.** Amperometric responses of rGO/GCE, CuO/rGO/GCE, NiO/rGO/GCE and NiO/CuO/rGO/GCE to successive injections of 50 μM glucose. Applied potential: 0.5 V.

*3.3. Optimization of experimental conditions*

The performance of NiO/CuO/rGO/GCE obtained at different electrodeposition time (60, 120, 180, 240, 300 s) was studied by CV in 0.1 M NaOH with 2 mM glucose involved (Fig. 5), because the

number and morphology of NiO/CuO/rGO nanocomposites on electrode depend on the electrodeposition time. When the electrodeposition time was 60 s, the oxidation current of glucose was low, probably because of relatively small amount of NiO/CuO nanoparticles electrodeposited on rGO surface. After 60 s, the anodic peak current became larger with electrodeposition time extended since the number of electrodeposited NiO/CuO nanoparticles increased. A largest current was observed at the electrodeposition time of 240 s. With the further increase of electrodeposition time to 300 s, a relatively reduced anodic peak current and positively shifted anodic peak potential were obtained. This phenomenon can be ascribed to the compact and thick NiO/CuO nanoparticles formed, which were unbeneficial for mass and electron transport during the glucose oxidation process. Therefore, 240 s of the electrodeposition time was chosen in this work due to the best catalytic performance for glucose oxidation.

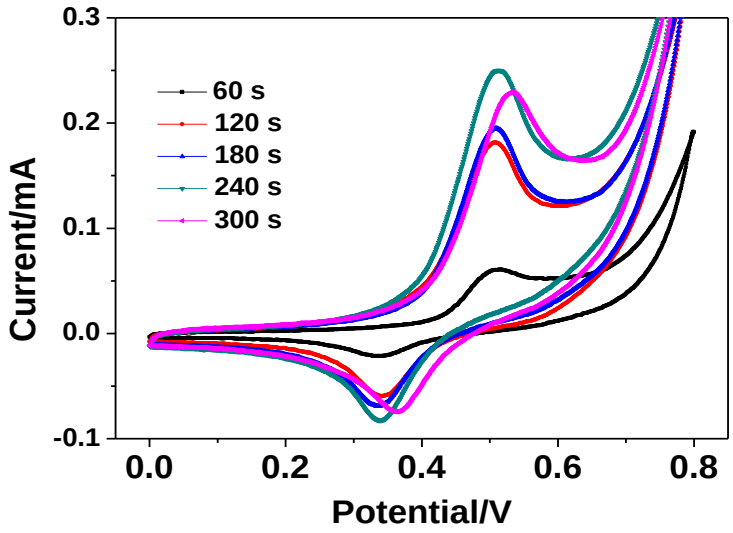


**Figure 5.** CVs of 2 mM glucose at the NiO/CuO/rGO/GCE obtained at different electrodeposition time.

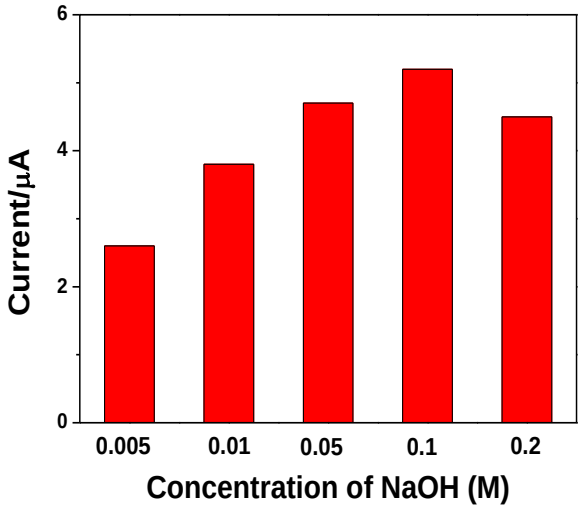


**Figure 6.** The current response of NiO/CuO/rGO/GCE toward 50 μM glucose at 0.50 V under different NaOH concentrations.

The influence of NaOH concentration was studied on amperometric measurements for detecting 50 μM glucose. As shown in Fig. 6, the amperometric currents increased correspondingly with the increase of NaOH concentration from 0.005 to 0.1 M. Afterwards, the amperometric currents lowered with the further increase of concentration in the range of 0.1～0.2 M. To ensure the largest detection sensitivity, here, the concentration of NaOH with 0.1 M was chosen as the optimal electrolyte solution.

The influence of applied potential was systemically investigated on the amperometric current of the NiO/CuO/rGO/GCE to glucose. Fig. 7 exhibits amperometric current of NiO/CuO/rGO/GCE to successive additions of 50 μM glucose at the potential range from +0.3 to +0.6 V with a settle interval of 0.1 V. Obviously, the amperometric current increased with the increase of applied potential from +0.3 to +0.5 V. When the applied potential further increased to +0.6 V, the amperometric current of glucose was nearly equal to that at +0.5 V, but the blank current enhanced distinctly compared to +0.5 V. It is well known that high applied potentials will result in poor selectivity for glucose sensing because the interference substance can be oxidized simultaneously with glucose. Therefore, an applied potential of +0.5 V was used for glucose detection to ensure enough detection sensitivity and selectivity.

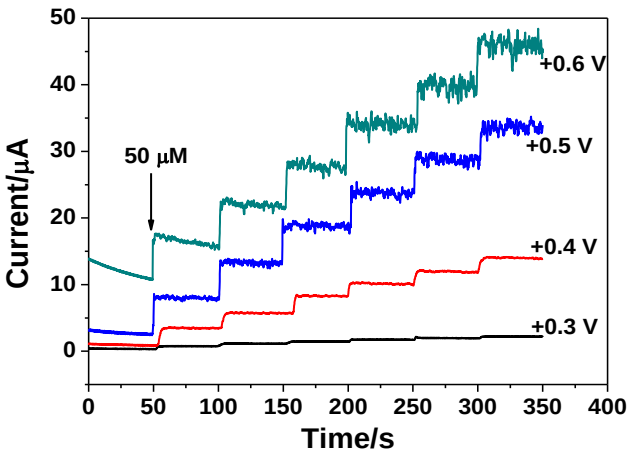


**Figure 7.** Amperometric currents of NiO/CuO/rGO/GCE to the successive injections of 50 μM glucose at different applied potentials.

*3.4. Amperometric determination of glucose and interference test*

The response of NiO/CuO/rGO/GCE toward various concentrations of glucose was first investigated using CV technique. Fig. 8a shows the CVs of NiO/CuO/rGO/GCE in 0.1 M NaOH with various concentrations of glucose (0 to 10 mM) involved. As observed, the anodic peak current corresponding to oxidation of glucose is found to increase linearly with the glucose concentration (inset of Fig. 8a), indicating the potential prospect for glucose sensing analysis. Under optimal conditions, amperometric currents to successive injections of glucose into stirring NaOH solution were performed. Fig. 8b displays the amperometric current of the NiO/CuO/rGO/GCE for injections of

glucose to increasing concentrations in 0.1 M NaOH at 0.5 V. It can be seen that steady amperometric currents increase correspondingly with the concentration of glucose. The required time for achieving a 90% of the steady current upon addition of glucose is less than 3 s, demonstrating fast and sensitive glucose oxidation at NiO/CuO/rGO/GCE. As shown in Fig 8c, the current response is proportional to the concentration of glucose over the range from 5 μM to 4.85 mM with a correlation coefficient of 0.9942 and a slope of 73.92 μA $mM^{-1}$. A sensitivity of 1046 μA $mM^{-1}$ $cm^{-2}$ is obtained for the NiO/CuO/rGO/GCE based glucose sensor. This value is higher than 79.3, 285, 622.2, 45.7, 223.39 μA $mM^{-1}$ $cm^{-2}$ for the transition-metal based non-enzymatic glucose sensor using materials of $CoO_x$NPs/ERGO [16], $Cu_2O/NiO_x$/GO [20], CuO microspheres [36], Graphene/pectin-CuNPs [37] and $Ni(OH)_2$ hollow spheres [33]. The limit of detection (LOD) is 0.5 μM at the signal/noise value of 3 (S/N=3).

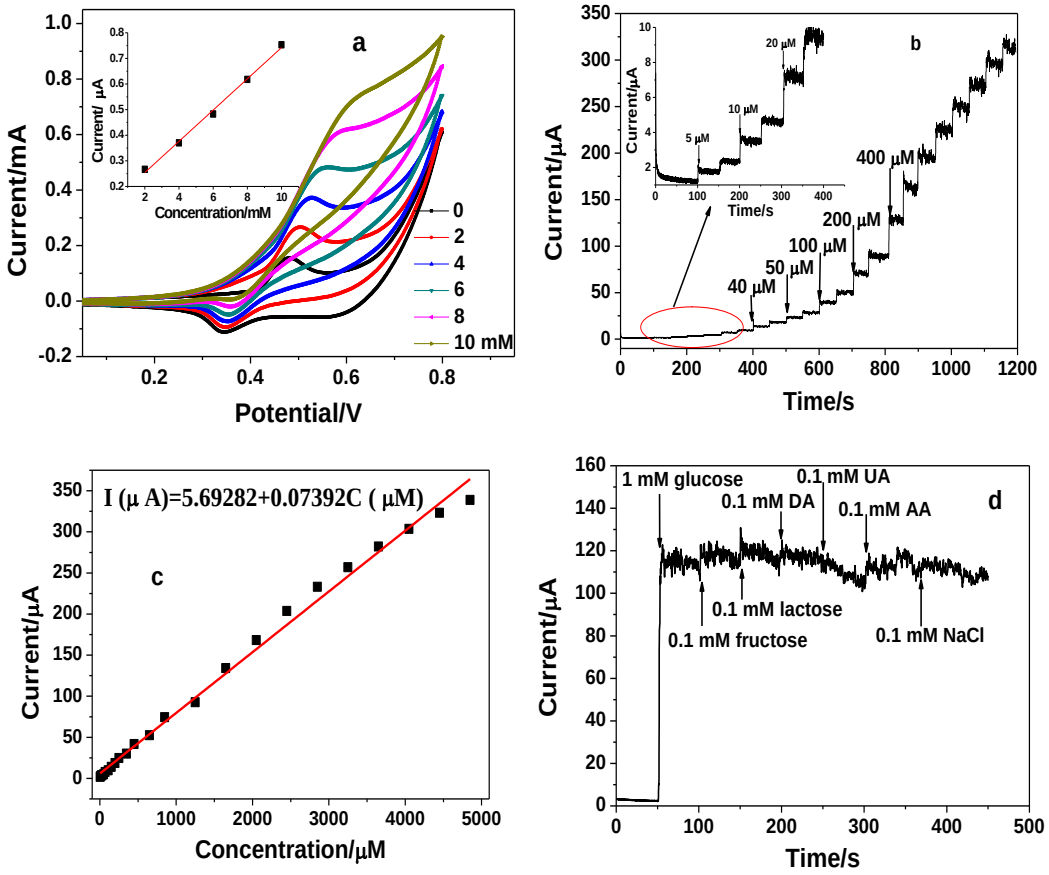


**Figure 8.** (a) The CVs of NiO/CuO/rGO/GCE in 0.1 M NaOH with various concentrations of glucose (0 to 10 mM) involved. (b) Amperometric current of the NiO/CuO/rGO/GCE for injections of glucose to increasing concentrations in 0.1 M NaOH at 0.5 V, (b) The corresponding calibration curve obtained from Fig. 9b. (d) Amperometric response of NiO/CuO/rGO/GCE to addition of 1 mM glucose in 0.1 M NaOH against additions of 0.1 mM interference: fructose, lactose, DA, UA, AA and NaCl at applied potential of 0.5 V.

The comparison of non-enzymatic glucose sensing performances using different nanomaterials from literature and our present work is shown in Table 1. Obviously, the performance of this

NiO/CuO/rGO sensor is nearly comparable to other nickel and copper based non-enzymatic glucose biosensors in view of low detection potential, high sensitivities, wide linear range and the low LOD. We attribute the favorable electrochemical sensing performance to the coordination effect of NiO/CuO binary catalyst, the high conductivity of graphene support, and the intimate contact between the nanocomposites and the current collector by direct electrodeposition method, which facilitates highly efficient biocatalyst of NiO/CuO easily accessing to glucose, thereby enhancing amperometric response of glucose.

Anti-interference ability is a key parameter for evaluating the selectivity of glucose biosensor. Some substance coexisting with glucose in biological samples, such as dopamine (DA), ascorbic acid (AA), uric acid (UA), fructose, lactose and NaCl, usually interfere with the detection signal of glucose. In human blood, the concentration of glucose is 30 to 50 times higher that that of common interferents. Here, the interference test regarding 0.1 mM interfering species with 1 mM glucose were evaluated to investigate the selectivity. Fig. 8d exhibits amperometric response of NiO/CuO/rGO/GCE to addition of 1 mM glucose in 0.1 M NaOH against additions of 0.1 mM interference: fructose, lactose, DA, UA, AA and NaCl. A significant glucose current response was observed compared to the other six interferents. All the interfering species generated current responses with less than 8% of glucose signal. Therefore, the present NiO/CuO/rGO nanocomposites electrode exhibited acceptable selectivity.

**Table 1.** The comparison of non-enzymatic glucose sensing performances using different nanomaterials.

| Electrode materials | Potential (V) | Sensitivity ($\mu A\ mM^{-1}\ cm^{-2}$) | Linear range | LOD ($\mu M$) | Reference |
|---|---|---|---|---|---|
| $CoO_x$NPs/ERGO | +0.60 | 79.3 | 0.01-0.55 mM | 2 | 16 |
| Graphene/NiO | +0.40 | 1571 | 0.005-2.8 mM | 1 | 17 |
| $Cu_2O/NiO_x$/GO | +0.6 | 285 | 0.002-0.87 mM | 0.4 | 20 |
| Ni-Co NSs/RGO | +0.50 | 1773.61 | 0.01-2.65 | 3.79 | 21 |
| $Ni(OH)_2$ hollow spheres | +0.45 | 223.39 | 0.8749 μM-7.781 mM | 0.1 | 33 |
| CuO microspheres | +0.50 | 622.2 | 0.005-7.95 mM | 1 | 36 |
| Graphene/pectin-CuNPs | +0.4 | 45.7 | 0.01-5.5 mM | 2.1 | 37 |
| CuONPs-graphene | +0.6 | 1065 | 0.001-8 mM | - | 38 |
| NiO/CuO/rGO | +0.50 | 1046 | 0.005-4.85 mM | 0.5 | This work |

### *3.5. Repeatability, reproducibility and stability of the NiO/CuO/rGO modified electrode*

To investigate the reproducibility of modified electrode toward electrooxidation of glucose, the current responses of six NiO/CuO/rGO electrodes prepared independently under the same conditions were compared. The results for amperometric determination of 50 μM glucose at +0.50 V showed a relative standard deviation (RSD) of only 4.6%. In addition, six measurements of 50 μM glucose using the same electrode yielded a RSD of 3.2%, indicating excellent electrode reproducibility. The long-term stability of developed electrode was studied by measuring its current response after one-month storage. The results showed only 6.8% decrease in the current response to 50 μM glucose.

### *3.6. Application in real sample analysis*

To verify the practical application of the developed sensor, the NiO/CuO/rGO nanocomposites electrode was used for the determination of glucose spiked in the human urine sample. The human urines spiked with 10 mM and 20 mM standard solution of glucose were labeled with sample 1 and 2, respectively. The amperometric current was measured by injection of 10 μL urine samples into 10 mL 0.1 mol $L^{-1}$ stirring NaOH solution at applied potential of +0.5 V. The standard addition method was used to obtain the recovery test. The results are shown in Table 2. The recovery for sample 1 and sample 2 is 104% and 98.0%, respectively, indicating high accuracy for determination of glucose in urine samples.

**Table 2**. Amperometric determination of glucose spiked in human urine samples (n=4).

| Urine samples | Spiked (μM) | Found (μM) | R.S.D (%) | Recovery (%) |
|---|---|---|---|---|
| Sample 1 | 10.0 | 10.4 | 2.64 | 104 |
| Sample 2 | 20.0 | 19.6 | 2.08 | 98.0 |

## 4. CONCLUSIONS

We have fabricated rGO supported binary catalyst of NiO/CuO on electrode by a direct electrochemical method and studied its application in enzyme-free glucose sensing. The NiO/CuO/rGO nanocomposites exhibited superior electrocatalytic activities towards oxidation of glucose compared to that of their monometallic oxide counterparts loaded on rGO surface. The improved electrochemical performance was attributed to the coordination effect of NiO/CuO binary catalyst, the excellent conductivity of rGO sheets, and the intimate contact between the nanocomposites and the current collector by direct electrodeposition method. The NiO/CuO/rGO based glucose sensor possessed good analytical performance, excellent reproducibility and stability, as well as good selectivity.

ACKNOWLEDGEMENTS
This work was supported by the Grants from the National Natural Science Foundation of China (21105002, 21273010), the fund project for Young Scholar sponsored by Henan province (14HASTIT012, 13HASTIT014, 2013GGJS-147) and for Henan Key Technologies R&D Program (122102310516, 12B150002).

## References

1. A. Heller, B. Feldman, *Chem. Rev*., 108 (2008) 2482.
2. X. Shi, W. Gu, B. Li, N. Chen, K. Zhao, Y. Xian, *Microchim. Acta*, 181 **(**2014) 1.
3. G. Wang, X. He, L. Wang, A. Gu, Y. Huang, B. Fang, B. Geng, X. Zhang, *Microchim. Acta*, 180 (2013) 161.
4. X. Chen, G. Wu, Z. Cai, M. Oyama, X. Chen, *Microchim. Acta* 181 (2014) 689.
5. L.C. Clark, C. Lyons, *Ann. NY Acad. Sci.*, 148 (1962) 133.
6. X. Niu, M. Lan, H. Zhao, C. Chen, *Anal. Chem*., 85 (2013) 3561.
7. S. Park, H. Booh, T.D. Chung, *Anal. Chim. Acta*, 556 (2006) 46.
8. M.M. Rahman, A.J.S. Ahammad, J.H. Jin, S.J. Ahn, J.J. Lee, *Sensors*, 10 (2010) 4855.
9. Q. Wang, Q. Wang, K. Qi, T. Xue, C. Liu, W. Zheng, X. Cui, *Anal. Methods*, 7 (2015) 8605.
10. J.H. Yuan, K. Wang, X.H. Xia, *Adv. Funct. Mater.*, 15 (2005) 803.
11. H. Shu, G. Chang, J. Su, L. Cao, Q. Huang, Y. Zhang, T. Xia, Y. He, *Sens. Actuators B*, 220 (2015) 331-339.
12. R. Ding, J. Liu, J. Jiang, J. Zhu, X. Huang, *Anal. Methods*, 4 (2012) 4003.
13. L. Zhao, G. Wu, Z. Cai, T. Zhao, Q. Yao, X. Chen, *Microchim. Acta*, 182 (2015) 2055.
14. C. Y. Ko, J. H. Huang, S. Raina, W. P. Kang, *Analyst*, 138 (2013) 3201.
15. S. Sun, Y. Sun, A. Chen, X. Zhang, Z. Yang, *Analyst*, 140 (2015) 5205.
16. S.J. Li, J.M. Du, J. Chen, N.N. Mao, M.J. Zhang, H. Pang, *J. Solid State Electrochem*., 18 (2014) 1049.
17. S.J. Li, N. Xia, X.L. Lv, M.M. Zhao, B.Q. Yuan, H. Pang, *Sens. Actuators B*, 190 (2014) 809.
18. A.J. Wang, J.J. Feng, Z.H. Li, Q.C. Liao, Z.Z. Wang, J.R. Chen, *CrystEngComm*., 14 (2012) 1289.
19. S.M. El-Refaei, M.M. Saleh, M.I. Awad, *J. Power Sources*, 223 (2013) 125.
20. B. Yuan, C. Xu, L. Liu, Q. Zhang, S. Ji, L. Pi, D. Zhang, Q. Huo, *Electrochim. Acta*, 104, (2013) 78.
21. L. Wang, X. Lu, Y. Ye, L. Sun, Y. Song, *Electrochim. Acta*, 114 (2013) 484.
22. W.D. Zhang, J. Chen, L.C. Jiang, Y.X. Yu, J.Q. Zhang, *Microchim. Acta*, 168 (2010) 259.
23. A.K. Geim, K.S. Novoselov, *Nat. Mater*., 6 (2007) 183.
24. A.K. Geim, *Science* 324 (2009) 1530.
25. J. Luo, H. Zhang, S. Jiang, J. Jiang, X. Liu, *Microchim. Acta*, 177 (2012) 485.
26. S.J. Li, J.M. Du, Y.F. Shi, W.J. Li, S.R. Liu, *J. Solid State Electrochem*., 16 (2012) 2235.
27. C. Guo, H. Yang, Z. Sheng, Z. Lu, Q. Song, C. Li, *Angew. Chem. Int. Ed*., 49 (2010) 3014.
28. X.M. Feng, R.M. Li, Y.W. Ma, R.F. Chen, N.E. Shi, Q. L. Fan, W. Huang, *Adv. Funct. Mater*., 21 (2011) 2989.
29. H.L. Guo, X.F. Wang, Q.Y. Qian, F.B. Wang, X.H. Xia, *ACS Nano* 3 (2009) 2653.
30. M. Zhou, Y. Wang, Y. Zhai, J. Zhai, W. Ren, F. Wang, S. Dong, *Chem. Eur. J*., 15 (2009) 6116.
31. J. Yang, L.C. Jiang, W.D. Zhang, S. Gunasekaran, *Talanta* 82 (2010) 25.
32. D. Zhang, Y. Fang, Z. Miao, M. Ma, X. Du, S. Takahashi, J. Anzai, Q. Chen, *Electrochim. Acta*, 107 (2013) 656.
33. P. Lu, Q. Liu, Y. Xiong, Q. Wang, Y. Lei, S. Lu, L. Lu, L. Yao, *Electrochim. Acta*, 168 (2015) 148.
34. S.J. Li, Y. Xing, G.F. Wang, *Microchim. Acta*, 176 (2012) 163.

35. L.C. Jiang, W.D. Zhang, *Biosens Bioelectron*., 25 (2010) 1402.
36. Y. Fan, X. Yang, Z. Cao, S. Chen, B. Zhu, *J. Appl. Electrochem*., 45 (2015) 131.
37. V. Mani, R. Devasenathipathy, S.M. Chen, S.F. Wang, P. Devi, Y. Tai, *Electrochim. Acta*, 176, (2015) 804.
38. Y.W. Hsu, T.K. Hsu, C.L. Sun, Y.T. Nien, N.W. Pu, M.D. Ger, *Electrochim. Acta*, 82 (2012) 152.